Microporous and Mesoporous Materials 169 (2013) 176–179

Contents lists available at SciVerse ScienceDirect

Microporous and Mesoporous Materials

journal homepage: www.elsevier.com/locate/micromeso

Short Communication

High xenon/krypton selectivity in a metal-organic framework with small pores and strong adsorption sites

Youn-Sang Bae [a,*], Brad G. Hauser [b], Yamil J. Colón [c], Joseph T. Hupp [b], Omar K. Farha [b,*], Randall Q. Snurr [c]

[a] Department of Chemical and Biomolecular Engineering, Yonsei University, 262 Seongsanno, Seodaemun-gu, Seoul 120-749, South Korea
[b] Department of Chemistry and International Institute for Nanotechnology, Northwestern University, 2145 Sheridan Road, Evanston, IL 60208, USA
[c] Department of Chemical and Biological Engineering, Northwestern University, 2145 Sheridan Road, Evanston, IL 60208, USA

ARTICLE INFO

Article history:
Received 17 September 2012
Received in revised form 8 November 2012
Accepted 9 November 2012
Available online 22 November 2012

Keywords:
Xenon
Krypton
Rare gases
Metal-organic framework (MOF)
Separation

ABSTRACT

Separation of Xe/Kr mixtures was studied in two copper-paddlewheel metal-organic framework materials, MOF-505 and HKUST-1. For MOF-505, which has small pores with strong adsorption sites, high Xe/Kr selectivities (9–10) are obtained from breakthrough measurements and grand canonical Monte Carlo (GCMC) simulations. The consistent results from both techniques suggest that MOF-505 is a promising candidate for Xe/Kr separation. For HKUST-1, which has small octahedral pores, only modest Xe/Kr selectivities (4.5) are observed from breakthrough measurements, although the GCMC simulations predicted unusually high selectivities at low loadings.

1. Introduction

Separation of xenon and krypton mixtures is industrially important, since both gasses are rare in nature but have several industrial uses including medical applications (e.g., imaging, anesthesia and neuroprotection), commercial lighting (e.g., fluorescent signs, desk stand and airport runway lights), and propellants in ion propulsion engines [1]. Currently, an 80/20 molar mixture of krypton–xenon is obtained as a by-product in cryogenic air separations and must undergo further cryogenic distillation to produce pure streams of xenon and krypton [2]. However, cryogenic distillation is energy- and capital-intensive [3].

Adsorptive separation, such as in pressure swing adsorption (PSA), is often considered as an energy- and cost-effective alternative to distillation and is widely used in the separation and purification of various gas mixtures. A key step in the design of PSA processes is the choice of a highly selective adsorbent with a high capacity [4]. Metal-organic frameworks (MOFs) have recently shown promise as adsorbents for gas separation and purification [5–11] due to their extremely high surface areas, tailorable pore structures, adjustable chemical functionalities and structural stability [12–14]. Müller et al. [6] published an experimental report on the selective adsorption of Xe over Kr using two of the most studied MOFs, IRMOF-1 and HKUST-1. Later, Greathouse et al. [15] computationally demonstrated that IRMOF-1 selectively adsorbs Xe atoms from Xe/Kr and Xe/Ar mixtures. Recently, Sikora et al. [16] generated >137,000 hypothetical MOFs from a library of chemical building blocks and screened them for Xe/Kr separation using a high-throughput computational method. They showed that MOFs with tube-like pores just large enough for a xenon atom to pass through are ideal for Xe/Kr separation. Also, Gurdal and Keskin [17] and Van Heest et al. [18] screened MOFs computationally for performance in several binary noble gas separations. To date, however, experimental studies on the separation of Xe/Kr mixtures by MOFs are scarce, and only a small number of experimental reports can be found [19–22]. Thallapally and co-workers reported that Ni/DOBDC has a significantly higher Xe adsorption capacity than MOF-5 and shows higher Xe/Kr selectivity than HKUST-1 and activated carbon [19,20]. They also demonstrated that a partially fluorinated MOF shows an unusual selectivity for Kr over Xe at temperatures below 273 K [21].

In this work, we performed a combined experimental and computational study on two copper-paddlewheel MOFs, MOF-505 and HKUST-1, as a follow-up to the previous computational study by Ryan et al. [23]. The MOF structures are shown in Fig. 1. Ryan et al. computationally screened eight existing MOFs for Xe/Kr separation at 273 K. Among the eight MOFs, Pd-MOF with small pores was predicted to have the highest Xe/Kr selectivity (18–19) at 0.1–

* Corresponding authors. Tel.: +82 2 2123 2755; fax: +82 2 312 6401.
E-mail addresses: mowbae@yonsei.ac.kr (Y.-S. Bae), o-farha@northwestern.edu (O.K. Farha).

1387-1811/$ - see front matter
http://dx.doi.org/10.1016/j.micromeso.2012.11.013

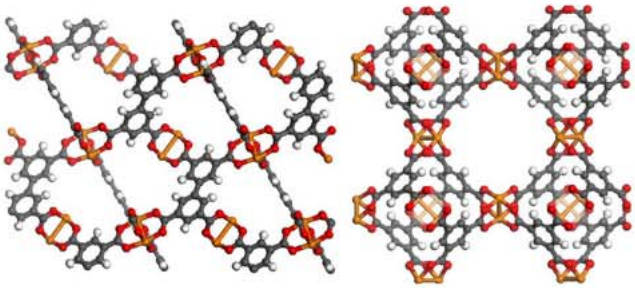

Fig. 1. Framework structures of MOF-505 (left) and HKUST-1 (right).

30 bar but showed significantly lower Xe and Kr uptake values than the other MOFs. For HKUST-1, the predicted Xe/Kr selectivity was high (17) at 0.1 bar but was modest (5–8) at 1–5 bar, which are typical PSA pressures. Compared with HKUST-1, MOF-505 showed higher selectivity (9–11) and larger uptake values at the typical PSA pressure range, which was ascribed to the smaller cavity size of MOF-505. Based on their simulation results, Ryan et al. suggested that MOF-505 is the best material among the eight MOFs studied considering both Xe/Kr selectivity and Xe capacity. The objective of the present study is to verify these computational predictions by performing packed-column breakthrough measurements, as well as some additional molecular simulations.

2. Experiments

MOF-505 was synthesized using a slight modification of a published procedure [24]. The obtained sample was activated at 393 K under nitrogen flow for 12 h then 473 K for an additional 12 h. HKUST-1 was synthesized using a slight modification of a published procedure [25]. The resulting sample was activated at 373 K under nitrogen flow for 6 h then 423 K for an additional 12 h. The activated samples were pelletized using a manual pellet press (Parr Instrument Company). The pellets were then carefully crushed and sieved to obtain particles with diameters between 600 and 1000 μm. The pelletized samples showed similar but slightly lower surface areas than the as-synthesized samples (see the Supporting Information).

Powder X-ray diffraction (PXRD) patterns were recorded with a Rigaku XDS 2000 diffractometer using nickel-filtered Cu Kα radiation (λ = 1.5418 Å) over a range of 5 < 2θ < 35 . Thermogravimetric analyses (TGA) were performed on a Mettler–Toledo TGA/SDTA851e. Nitrogen isotherms at 77 K were measured on a Micromeritics TriStar 3020.

The breakthrough measurements of a 20:80 mixture of xenon and krypton on MOF-505 and HKUST-1 were performed using a slight modification of a published procedure [26]. Adsorbed amounts of xenon and krypton were calculated by integrating the resulting breakthrough curves.

The grand canonical Monte Carlo (GCMC) simulations were performed to simulate the adsorption of a 20:80 mixture of xenon and krypton on MOF-505 and HKUST-1 at 298 K using a published method [23]. The details of the experimental and computational methods are described in Supporting Information.

3. Results and discussion

Using GCMC simulations, Ryan et al. [23] identified MOF-505 as a promising adsorbent due to its high Xe/Kr selectivity (9–11) over the typical range of operating pressures for PSA (1–10 bar) and its good capacity. We sought to verify if these computationally obtained selectivities can be attained experimentally from dynamic breakthrough measurements. Fig. 2a shows the resulting breakthrough curves for 20:80 mixtures of Xe and Kr in MOF-505 pellets at total mixture pressures of 0.5 and 1 bar. A clear difference in breakthrough time between Xe and Kr was observed. While pure Kr elutes instantly from the column, Xe shows considerable retention. The Kr concentration at the column outlet slightly exceeds the feed concentration because the more strongly adsorbed Xe molecules displace the already adsorbed Kr molecules. As the column is saturated with Xe and Kr, the outlet concentrations of both components approach the feed concentrations. By comparing the dashed and continuous lines in Fig. 2a, we can see that the breakthrough time of Xe becomes shorter as the total mixture pressure decreases. This is an expected result, because the adsorbed amount decreases with decreasing pressure.

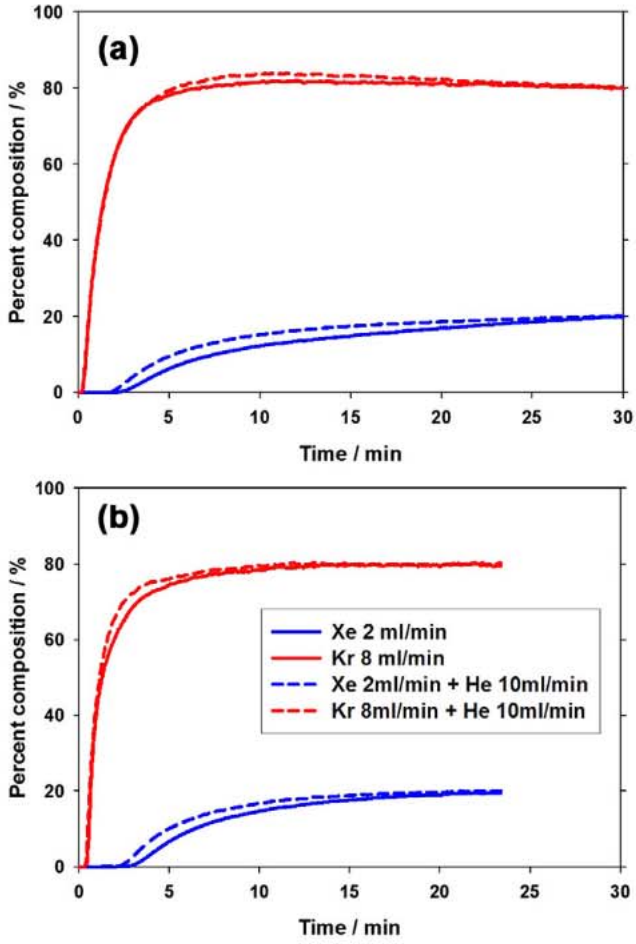

Fig. 2. Breakthrough curves for 80:20 mixture of Kr and Xe in (a) MOF-505 pellets and, (b) HKUST-1 pellets at room temperature. Each figure presents two breakthrough runs: one without He carrier (total flow rate = 10 ml/min, total mixture pressure = 1 bar) and one with 10 ml/min of He carrier (total flow rate = 20 ml/min, total mixture pressure = 0.5 bar).

The adsorbed amounts of Xe and Kr at mixture conditions can be calculated by integrating the areas above the breakthrough curves. The adsorption selectivity of Xe over Kr ($S_{Xe/Kr}$) can be calculated from the standard definition, $S_{Xe/Kr} = (x_{Xe}/x_{Kr})\cdot(y_{Kr}/y_{Xe})$. Here, x and y are the mole fractions of the adsorbed and bulk phases, respectively. Fig. 3 shows the resulting Xe and Kr uptake values and Xe/Kr selectivities at two different total mixture pressures (0.5 and 1 bar) for a 20:80 mixture of Xe and Kr in MOF-505. The obtained selectivities are high (9–10) and close to the simulated selectivity at 273 K from Ryan et al. [23] although they are measured at room temperature. To make a better comparison with simulation, we performed GCMC simulations to calculate

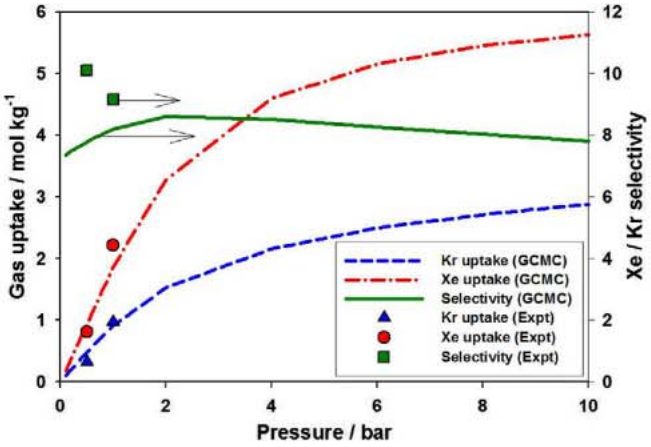

Fig. 3. Experimental and simulated adsorption isotherms for a 20:80 mixture of Xe and Kr in MOF-505 at 298 K. Experimental data were obtained from breakthrough measurements.

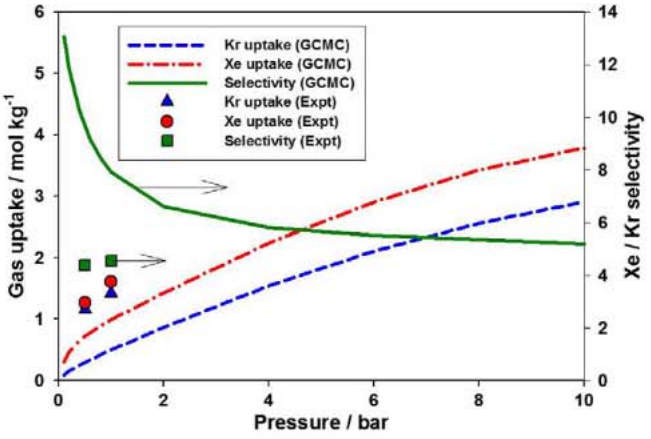

Fig. 4. Experimental and simulated adsorption isotherms for a 20:80 mixture of Xe and Kr in HKUST-1 at 298 K. Experimental data were obtained from breakthrough measurements.

the mixture isotherms and selectivity at 298 K. As presented in Fig. 3, the simulated data match reasonably well with the experimental isotherms and selectivity. It is remarkable that consistent results were obtained from two totally different techniques. The slightly higher experimental selectivities compared to the simulated ones may come from some possible defects in the MOF sample, errors in the uptake values from the breakthrough measurements, or inaccuracy in the model used for the GCMC simulations. It should also be noted that the selectivities may contain higher errors than the isotherms because the errors from two isotherms are accumulated. The measured selectivity (9–10) is among the highest Xe/Kr selectivities reported. It is considerably higher than the experimental selectivities recently reported for other MOFs and carbon adsorbent at similar conditions: Ni/DOBDC (4), HKUST-1 (2.6) and activated carbon (2.8) [20]. Also, MOF-505 shows high Xe uptake (2.2 mol/kg) at a partial pressure of 0.2 bar (total mixture pressure = 1 bar). From pure-component adsorption at room temperature, the uptake values of Xe at 0.2 bar by Ni/DOBDC, MOF-5 and activated carbon were 1.5, 0.5 and 1.5 mol/kg, respectively [19]. These results suggest that MOF-505 is a promising candidate for Xe separation from Xe/Kr mixtures. This may be attributed to the pore confinement effect of small pores (4.8, 7.1 and 9.5 Å). These small pores serve as strong adsorption sites, especially for Xe which adsorbs more strongly than Kr due to van der Waals interactions and its higher polarizability.

Ryan et al. [23] also performed similar simulations for HKUST-1 at 273 K. Their mixture adsorption simulation for HKUST-1 predicted unusually high Xe/Kr selectivity (17) at 0.1 bar, which was ascribed to small octahedral pockets (5.0 Å) that can accommodate only one atom of Xe or Kr. But, the selectivity decreased steeply as the pressure increased due to the adsorption in the larger pores (10.6–12.4 Å) and became modest (6–8) at higher pressures between 1 and 10 bar, which is the typical PSA pressure range. To compare with experiments at room temperature, we repeated the simulations for a 20:80 mixture of Xe and Kr at 298 K. As shown in Fig. 4, a similar trend with the results at 273 K is observed, but slightly lower selectivities are obtained: 13 at 0.1 bar and 5–8 at 1–10 bar. We also performed breakthrough measurements for 20:80 mixtures of Xe and Kr in HKUST-1 pellets at total mixture pressures of 0.5 and 1 bar (Fig. 2b). In Fig. 4, the resulting Xe and Kr uptake values and Xe/Kr selectivities are compared with the simulated data. Unlike MOF-505, the experimental Xe and Kr uptake values in HKUST-1 are higher than the simulated values. Moreover, both Xe and Kr show similar uptake, and thus the resulting selectivities are modest (about 4.5) compared to the simulated ones (8–9.5) at similar conditions. Liu et al. [20] reported even lower Xe/Kr selectivity (2.6) for HKUST-1 from similar breakthrough measurements at similar conditions. The deviation in the experimental selectivities may come from possible defects in the HKUST-1 samples due to the hydrothermal instability or from differences in synthesis and activation. Considering the low BET surface area (1252 m^2/g) of the sample from Liu et al., we can speculate that their sample has the octahedral pockets blocked, which would explain the lower selectivity. Also, we hypothesize the following explanation for the discrepancy between the experimental and simulated selectivities. For the GCMC simulations, the high Xe/Kr selectivities at low pressures come from the dominant adsorption of Xe in the small octahedral pockets which can accommodate only one Xe or Kr atom. For the breakthrough measurements, the situation may be different because the measurement reflects both equilibrium and kinetic effects. In a packed column, the weaker adsorbate Kr moves down the column faster than Xe and thus is initially adsorbed inside of small octahedral pockets toward the exit of the column. When Xe reaches the downstream end of the column, the stronger adsorbate Xe pushes out the Kr adsorbed at these small octahedral pockets. Hence, in the experimental breakthrough experiments, both Xe and Kr are adsorbed in the same octahedral pockets within a short interval of time. As a result, these octahedral pockets do not have as strong an effect on Xe/Kr selectivity as is observed in the simulations. The higher experimental uptake values compared to those from simulations may come from slow movement of Xe and Kr atoms due to the small apertures of the octahedral pockets, which results in long breakthrough times. These combined equilibrium and kinetic experimental results indicate that HKUST-1 is a less promising candidate for Xe/Kr separation, although the equilibrium GCMC simulations showed unusually high selectivities at low loadings.

4. Conclusions

Breakthrough measurements and GCMC simulations have shown that MOF-505 is a promising candidate for Xe separation from Xe/Kr mixtures. The measured selectivity (9–10) is among the highest Xe/Kr selectivities reported to date. We attribute the high selectivity to the pore confinement effect of the small pores (4.8, 7.1 and 9.5 Å). On the other hand, our breakthrough measurements show that HKUST-1 has modest Xe/Kr selectivities (4.5). This work highlights that while GCMC simulation may provide useful suggestions for adsorption separations, kinetic effects can also

play a role, and breakthrough measurements are a useful method to test for this.

Acknowledgments

We gratefully acknowledge support from the U.S. Department of Energy (DEFG02-08ER15967). This research has been performed as a cooperation Project no. KK-1201-F0 (Synthesis of Porous Hybrids and Their Applications) and supported by the Korea Research Institute of Chemical Technology (KRICT).

Appendix A. Supplementary data

Supplementary data associated with this article can be found, in the online version, at http://dx.doi.org/10.1016/j.micromeso.2012.11.013.

References

[1] S.C. Cullen, E.G. Gross, Science 113 (1951) 580–582.
[2] F.G. Kerry, Industrial Gas Handbook: Gas Separation and Purification, CRC Press, Boca Raton, Florida, 2007.
[3] J. Izumi, in: S.M. Auerbach, K.A. Carrado, P.K. Dutta (Eds.), Waste Gas Treatment using Zeolites in Nuclear-Related Industries, Handbook of Zeolites Science and Technology, Marcel Dekker, New York, 2003.
[4] R.T. Yang, Adsorbents: Fundamentals and Applications, John Wiley & Sons, Inc., Hoboken, 2003.
[5] R.Q. Snurr, J.T. Hupp, S.T. Nguyen, AIChE J. 50 (2004) 1090.
[6] U. Mueller, M. Schubert, F. Teich, H. Puetter, K. Schierle-Arndt, J. Pastre, J. Mater. Chem. 16 (2006) 626.
[7] L. Pan, D.H. Olson, L.R. Ciemnolonski, R. Heddy, J. Li, Angew. Chem. Int. Ed. 45 (2006) 616.
[8] J.R. Li, R.J. Kuppler, H.C. Zhou, Chem. Soc. Rev. 38 (2009) 1477.
[9] M. Tagliabue, D. Farrusseng, S. Valencia, S. Aguado, U. Ravon, C. Rizzo, A. Corma, C. Mirodatos, Chem. Eng. J. 155 (2009) 553–566.
[10] S. Keskin, T.M. van Heest, D.S. Sholl, ChemSusChem 3 (2010) 879–891.
[11] J.R. Li, Y.G. Ma, M.C. McCarthy, J. Sculley, J.M. Yu, H.K. Jeong, P.B. Balbuena, H.C. Zhou, Coord. Chem. Rev. 255 (2011) 1791–1823.
[12] G. Férey, Chem. Soc. Rev. 37 (2008) 191.
[13] K.M. Thomas, Dalton Trans. (2009) 1487.
[14] J.L.C. Rowsell, O.M. Yaghi, Microporous Mesoporous Mater. 73 (2004) 3.
[15] J.A. Greathouse, T.L. Kinnibrugh, M.D. Allendorf, Ind. Eng. Chem. Res. 48 (2009) 3425–3431.
[16] B.J. Sikora, C.E. Wilmer, M.L. Greenfield, R.Q. Snurr, Chem. Sci. 3 (2012) 2217–2223.
[17] Y. Gurdal, S. Keskin, Ind. Eng. Chem. Res. 51 (2012) 7373–7382.
[18] T. Van Heest, S.L. Teich-McGoldrick, J.A. Greathouse, M.D. Allendorf, D.S. Sholl, J. Phys. Chem. C 116 (2012) 13183–13195.
[19] P.K. Thallapally, J.W. Grate, R.K. Motkuri, Chem. Commun. 48 (2012) 347–349.
[20] J. Liu, P.K. Thallapally, D. Strachan, Langmuir 28 (2012) 11584–11589.
[21] C.A. Fernandez, J. Liu, P.K. Thallapally, D.M. Strachan, J. Am. Chem. Soc. 134 (2012) 9046–9049.
[22] A.S. Dorcheh, D. Denysenko, D. Volkmer, W. Donner, M. Hirscher, Microporous Mesoporous Mater. 162 (2012) 64–68.
[23] P. Ryan, O.K. Farha, L.J. Broadbelt, R.Q. Snurr, AIChE J. 57 (2011) 1759–1766.
[24] B. Chen, N.W. Ockwig, A.R. Millward, D.S. Contreras, O.M. Yaghi, Angew. Chem. Int. Ed. 44 (2005) 4745–4749.
[25] S. Marx, W. Kleist, A. Baiker, J. Catal. 281 (2011) 76–87.
[26] Y.-S. Bae, C.Y. Lee, K.C. Kim, O.K. Farha, P. Nickias, J.T. Hupp, S.T. Nguyen, R.Q. Snurr, Angew. Chem. Int. Ed. 51 (2012) 1857–1860.